



OPEN ACCESS

EDITED BY

Jianbo Yang,
University of Minnesota Twin Cities,
United States

REVIEWED BY

Aileen Fernandez,
Yale University, United States
Benjamin Heng,
Macquarie University, Australia

*CORRESPONDENCE

Tingmei Chen
✉ tingmeichen@cqmu.edu.cn
Chengsen Chai
✉ chengsenchai@cqmu.edu.cn

[†]These authors have contributed equally to this work

RECEIVED 28 January 2023

ACCEPTED 24 April 2023

PUBLISHED 05 May 2023

CITATION

Yuan R, Zhang Y, Wang Y, Chen H, Zhang R, Hu Z, Chai C and Chen T (2023) GNPAT1 is a potential biomarker correlated with immune infiltration and immunotherapy outcome in breast cancer. *Front. Immunol.* 14:1152678. doi: 10.3389/fimmu.2023.1152678

COPYRIGHT

© 2023 Yuan, Zhang, Wang, Chen, Zhang, Hu, Chai and Chen. This is an open-access article distributed under the terms of the [Creative Commons Attribution License \(CC BY\)](https://creativecommons.org/licenses/by/4.0/). The use, distribution or reproduction in other forums is permitted, provided the original author(s) and the copyright owner(s) are credited and that the original publication in this journal is cited, in accordance with accepted academic practice. No use, distribution or reproduction is permitted which does not comply with these terms.

GNPNAT1 is a potential biomarker correlated with immune infiltration and immunotherapy outcome in breast cancer

Renjie Yuan^{1†}, Yulu Zhang^{1†}, Yange Wang¹, Hongling Chen¹, Ruiming Zhang¹, Zhiyuan Hu², Chengsen Chai^{1*} and Tingmei Chen^{1*}

¹Key Laboratory of Clinical Laboratory Diagnostics (Ministry of Education), College of Laboratory Medicine, Chongqing Medical University, Chongqing, China, ²Chinese Academy of Sciences (CAS) Key Laboratory of Standardization and Measurement for Nanotechnology, Chinese Academy of Sciences (CAS) Key Laboratory for Biomedical Effects of Nanomaterials and Nanosafety, Chinese Academy of Sciences (CAS) Center for Excellence in Nanoscience, National Center for Nanoscience and Technology, Beijing, China

Background: Glucosamine 6-phosphate N-acetyltransferase (GNPNAT1) is a crucial enzyme involving hexosamine biosynthesis pathway and is upregulated in breast cancer (BRCA). However, its biological function and mechanism on patients in BRCA have not been investigated.

Methods: In this study, the differential expression of GNPAT1 was analyzed between BRCA tissues and normal breast tissues using the Cancer Genome Atlas (TCGA) database and Gene Expression Omnibus (GEO) database, which was validated by quantitative real-time polymerase chain reaction, Western blot and immunohistochemistry. Then, the potential clinical value of GNPAT1 in BRCA was investigated based on TCGA database. Functional enrichment analyses, including Gene Ontology, Kyoto Encyclopedia of Genes and Genomes, Gene Set Variation Analysis, were performed to explore the potential signaling pathways and biological functions involved in GNPAT1 in BRCA. Tumor immune infiltration was analyzed using ESTIMATE, CIBERSORT and TISIDB database; and immune therapy response scores were assessed using TIDE. Finally, Western blot, Cell counting kit-8 and Transwell assay were used to determine the proliferation and invasion abilities of breast cancer cells with GNPAT1 knockdown.

Results: GNPAT1 was up-regulated in BRCA tissues compared with normal tissues which was subsequently verified in different cell lines and clinical tissue samples. Based on TCGA and GEO, the overexpression of GNPAT1 in BRCA contributed to a significant decline in overall survive and disease specific survive. Functional enrichment analyses indicated that the enriched pathways in high GNPAT1 expression group included citrate cycle, N-glycan biosynthesis, DNA repair, and basal transcription factors. Moreover, the overexpression of GNPAT1 was negatively correlated with immunotherapy response and the levels of immune cell infiltration of CD8+ T cells, B cells, natural killer cells,

dendritic cells and macrophages. Knockdown of GNPAT1 impairs the proliferation and invasion abilities of breast cancer cells.

Conclusion: GNPAT1 is a potential diagnostic, prognostic biomarker and novel target for intervention in BRCA.

KEYWORDS

GNPAT1, breast cancer, biomarker, tumor-infiltration immune cells, immune checkpoints inhibitors, immunotherapy response

1 Introduction

Breast cancer (BRCA) has surpassed lung cancer as the most commonly diagnosed malignancy worldwide, and it is the leading cause of cancer-related death among women (1). Breast cancer is a complex disease that displays a large degree of heterogeneity (2, 3). Due to the immunohistochemical expression of the following receptors: estrogen receptor (ER), progesterone receptor (PR) and human epidermal growth factor receptor 2 (HER2), this heterogeneous disease is categorized into three groups: hormone receptors (HR) positive, HER2 positive, and triple-negative (4). HR positive tumors are characterized by the presence of HR and the absence of HER2, hence these patients present ideal efficacy to hormone therapy (tamoxifen or aromatase inhibitors). HER2 positive breast cancer is an aggressive subtype, its standard first-line treatment consists of HER2 targeted therapy, including trastuzumab, and pertuzumab. Triple Negative Breast Cancers (TNBC), without the expression of HR, are a group with only chemotherapy and immunotherapy options (5). Despite significant improvements in the diagnosis and treatment of breast cancer, there are still a large number of patients who are resistant to therapy or relapse after treatment. Therefore, identifying a universal clinical biomarker and therapeutic target will benefit patients in BRCA.

Glucosamine 6-phosphate N-acetyltransferase (GNPAT1), also called GNA1, encodes a crucial enzyme catalyzing the formation of N-acetylglucosamine-6-phosphate from acetyl-CoA and the acceptor substrate glucosamine-6-phosphate (6, 7), which is an essential intermediate in hexosamine biosynthesis pathway (HBP). The end product of HBP is UDP-N-acetylglucosamine, and its expression level is known to affect protein O-GlcNAcylation by O-GlcNAc transferase. Previous studies found that GNPAT1 is a potential biomarker to predict sensitivity to radiotherapy of ER positive BRCA patients (8). Furthermore, researchers proved that GNPAT1 is a promising diagnostic and prognostic biomarker and correlates with immune infiltration in lung adenocarcinoma (9–11). However, its clinical value and potential mechanism in BRCA are still unclear.

In this study, we first analyzed the differential expression of GNPAT1 between BRCA tissues and normal breast tissues and elucidated its clinical implications based on the Cancer Genome Atlas (TCGA) and Gene Expression Omnibus (GEO) database, which was also confirmed by quantitative real-time polymerase chain reaction

(qRT-PCR), Western blot and immunohistochemistry (IHC). Furthermore, we investigated the correlation between GNPAT1 expression and its potential involved signaling pathways, immune infiltration levels and immunotherapy response. Additionally, Knockdown of GNPAT1 impairs the proliferation and invasion abilities of breast cancer cells. Based on these results, we could better understand the potential role of GNPAT1 in BRCA, and our study provided a new perspective of GNPAT1 for the potential diagnosis, prognosis and even treatment of patients in BRCA in the future.

2 Materials and methods

2.1 Data acquisition

The expression profiles and the corresponding clinical information of BRCA patients were downloaded from TCGA via GDC portal (<https://portal.gdc.cancer.gov/>). Two BRCA datasets (GSE10810 and GSE70591) were downloaded from the GEO database (<https://www.ncbi.nlm.nih.gov/geo/>). Then, we used TIMER 2.0 (<http://timer.cistrome.org/>) to analyze pan-cancer expression pattern of GNPAT1, and we used UCALAN (<http://ualcan.path.uab.edu/>) and HPA (<https://www.proteinatlas.org/>) to compare protein expression of GNPAT1 between BRCA tissues and normal tissues.

2.2 Receiver operating characteristic curves and survival analysis

ROC curves were used to evaluate the diagnostic efficiency of GNPAT1. We generated ROC curves using the “pROC” R package (12). Area under curve (AUC) was used as the following criteria: 0.50–0.60 = fail, 0.60–0.70 = poor, 0.70–0.80 = fair, 0.80–0.90 = good and 0.90–1 = excellent to evaluate diagnostic performance. Then, we defined patients with the expression level of GNPAT1 higher than median as the high_GNPAT1 group and the remainder as the low_GNPAT1 group. Survival statistics were plotted by GEPIA 2 database (<https://gepia2.cancer-pku.cn/>), K-M plotter database (<https://kmplot.com/>) and analyzed using the Log-Rank test. Cox regression model was applied for regression analysis.

2.3 Identification of differentially expressed genes and functional enrichment analysis

Firstly, the 1083 BRCA patients in TCGA were divided into two groups by the median expression level of GNPAT1. DEGs were identified using “DESeq2” R package (13). False positive results were corrected using the adjusted P value. The screening thresholds for differentially expressed genes (DEGs) were defined as follows: adjusted P value < 0.05 and $|\log_2(\text{fold change})| > 1$. Gene Ontology (GO) and Kyoto encyclopedia of genes and genomes (KEGG) analyses were conducted using the “clusterProfiler” R package (14). Adjusted P value < 0.05 is considered statistically significant in the enrichment results. Then, we applied Gene Set Variation Analysis (GSVA) to calculate enrichment scores in each patient for the 186 KEGG pathways described in the molecular signature database (MSigDB v7.5.1), as implemented in the “GSVA” R package (15). GSVA output was then submitted to “limma” to determine differentially expressed pathways (16).

2.4 Tumor immune infiltration analysis

We evaluated the levels of the immune cell infiltration, the stromal content, the stromal-immune comprehensive score and tumor purity for each BRCA sample by “ESTIMATE” R package (17). Then, a total of 22 immune cells were used to calculate the level of immune infiltration, and the relative enrichment score of these immune cells in breast cancer was assessed by “CIBERSORT” R package (18). We used TISIDB database (<http://cis.hku.hk/TISIDB/>) to determine the Spearman correlations between GNPAT1 expression and Tumor-infiltrating Immune cells (TILs), major histocompatibility complex (MHC) molecule abundance in BRCA.

2.5 Immunotherapy response analysis

Use the TIDE algorithm to calculate immunotherapy response score that constructed by Jiang et al. (19), which based on the mRNA expression signature. TIDE uses a set of markers to evaluate two different mechanisms of tumor immune escape, including the dysfunction of tumor infiltrating cytotoxic T lymphocytes (CTL) and the rejection of CTL by immunosuppressive factors. The high TIDE score means that immune checkpoint blocking therapy has poor efficacy.

2.6 Cell lines and cells culture

Human non-transformed mammary epithelial cell line MCF-10A and breast cancer cell lines, including MCF-7, ZR-75-1, SK-BR-3, MDA-MB-231, BT549, Hs578t, in this study were purchased from National Collection of Authenticated Cell Cultures (China). All cell lines were cultured under 37°C, 5% CO₂ condition.

2.7 RNA extraction and qRT-PCR

RNA was extracted from whole cell lysates with Trizol reagent (Takara, Japan) and was reverse-transcribed with the PrimeScriptTM RT reagent Kit (Takara, Japan) according to the instructions of manufacturer. All qRT-PCR was performed with the SYBR Premix Ex Taq II (TaKaRa, Japan). The primers were as follows: forward primer 5'- CACCATTGGCAATGAGCGGTTC-3' and reverse primer 5'- AGGTCTTTGCGGATGTCCACGT-3' for Actin Beta; forward primer 5'- ATTTGGGTCGCAGTTCTTG-3' and reverse primer 5'- TGCCTTGACATTCTCGATGGT-3' for Ubiquitin C; forward primer 5'-AGGGCCTCTACGGTTCCTGT-3' and reverse primer 5'-GTGTTGGGAAATGGCTGGA-3' for GNPAT1. Reference genes used in each qPCR run were Actin Beta and Ubiquitin C (20).

2.8 Western blot

Total protein was extracted by RIPA buffer (Beyotime, China) containing 1% PMSF (Beyotime, China) and was quantified using a BCA Kit (Beyotime, China) according to the instructions of the manufacturer. 40 mg of protein was fractionated by SDS-PAGE, transferred onto 0.45 μm PVDF membrane (Millipore, USA). The membranes were blocked with defatted milk powder (Biosharp, China) at room temperature for one hour and incubated with the appropriate primary antibodies. The specific primary antibodies against GNPAT1 (16282-1-AP, Proteintech, 1:1000), α-Tubulin (66031-1-Ig, Proteintech, 1:20000), c-Myc (67447-1-Ig, Proteintech, 1:5000), Cyclin D1 (WL01435a, Wanlei, 1:1000), Bcl-2 (BF9103, Affinity, 1:1000), Bax (2772, CST, 1:1000), E-cadherin (ET1607-75, Huabio, 1:1000), N-cadherin (ET1607-37, Huabio, 1:1000), Vimentin (BS1491, Bioworlde, 1:1000) were used and incubated at 4°C overnight. After being washed for three times in TBST, the membrane was incubated with corresponding HRP-conjugated secondary antibodies (BL001A and BL003A, Biosharp, 1:10000) at room temperature for one hour. Immunoblots were visualized by gel and blot imaging system (Bio-Rad, USA) with enhanced chemiluminescence assay (Millipore, USA).

2.9 Pathological sample collection and immunohistochemistry

A total of 16 pairs of paraffin-embedded breast cancer tissues and their matched para-tumor tissues were collected at the Pathology Department of the First Affiliated Hospital of Chongqing Medical University. These samples include 5 pairs of HR positive patients, 6 pairs of HER2 positive patients and 5 pairs of TNBC patients. Breast cancer tissues and para-tumor tissues were fixed in 10% neutralized formaldehyde for 24 hours and then embedded in paraffin. The paraffin-embedded samples were cut into 4-μm-thick sections. The primary antibody against GNPAT1 (16282-1-AP, Proteintech; 1:200) was incubated overnight at 4°C.

Afterwards, the slides were incubated with secondary antibody at room temperature for one hour and stained with DAB substrate, followed by hematoxylin counterstaining. IHC optical density scores were calculated to quantify protein expression in ImageJ (21).

2.10 Cell transfection

To generate MCF-7 and MDA-MB-231 cells with GNPAT1 knockdown, cells transfection was performed by Lipofectamine 2000 (Invitrogen, USA) according to the manufacturer's instructions. The siRNA targeting GNPAT1 and control siRNA were purchased from Tsingke Biotechnology Co., Ltd. (China). The sequences for siGNPAT1 are 5'-GAGUCAGAAUACAGCUACA(dT)(dT)-3'.

2.11 Cell counting kit-8 assay

The CCK-8 (Biosharp, China) assay was used to detect the cell proliferation ability. MCF-7 and MDA-MB-231 were seeded in 96-well plates at a density of 5×10^3 cells per well and 2×10^3 cells per well, respectively. The 10% CCK-8 reagent was added after incubating the cells for blank, 0, 24, 48 and 72h, measuring the optical density (OD) value at 450nm and 650nm one hour later. The OD values used for analysis have subtracted the average OD value of blank wells.

2.12 Transwell assay

The MCF-7 and MDA-MB-231 cells with good morphology and growth were selected, digested with trypsin, and resuspended in serum free medium for later use. Matrigel (1: 8 dilutions; Corning, USA), and 200 μ L of cell suspension containing 2×10^4 (MDA-MB-231) or 5×10^4 (MCF-7) cells were added to the upper layer of the Transwell chamber, and 600 μ L culture medium with 20% serum was added to the lower chamber. After culturing for 24h (MDA-MB-231) or 72h (MCF-7), invading cells were fixed, stained with

crystal violet, imaged, and counted by ImageJ (threshold range of cells counting: 180-infinity pixels²).

2.13 Bioinformatics analysis and statistical analysis

All analyses were done in R (v4.0.2) or GraphPad Prism (v9.4.0). The results of wet experiments were shown as mean \pm standard deviation, n = 3. The methods of computing statistical significance were presented in corresponding figure legends and p-value was annotated by the number of stars (*: p-value < 0.05; **: p-value < 0.01; ***: p-value < 0.001; ****: p-value < 0.0001). The flow diagram of this study was presented in Figure 1.

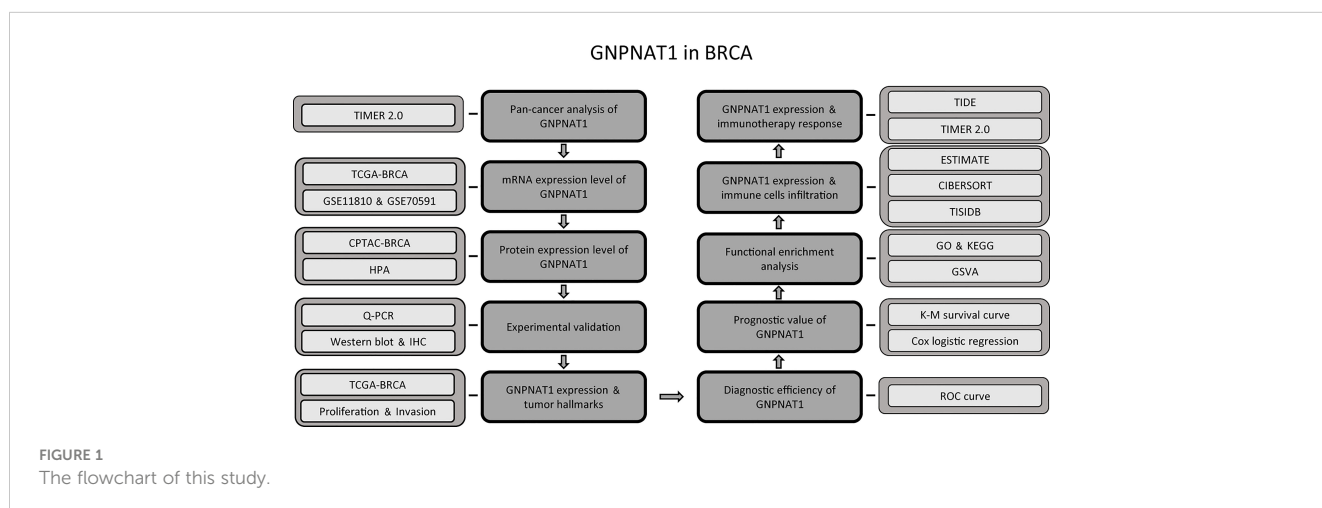
3 Results

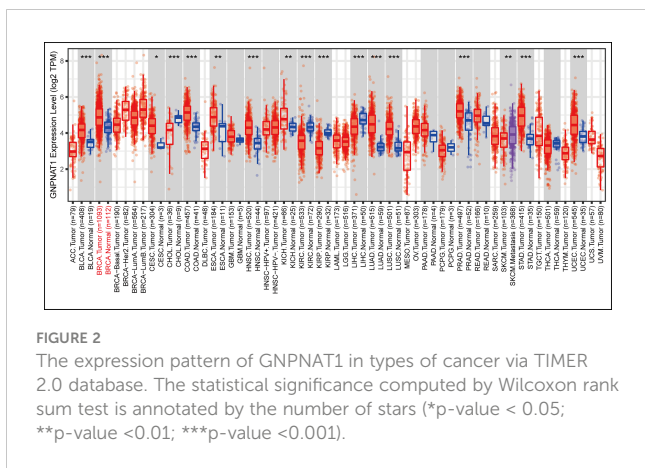
3.1 The expression of GNPAT1 in pan-cancers and BRCA

Initially, Comparing GNPAT1 expression between normal tissues and tumor samples from TCGA database, we found that GNPAT1 was significantly up-regulated in many types of cancer, including BRCA (Figure 2).

Then, we analyzed the mRNA expression level of GNPAT1 via TCGA cohort. The significant up-regulation of GNPAT1 expression was found in breast cancer tissues compared with normal tissues (Figure 3A). In addition, GNPAT1 was also highly expressed in 113 paired breast cancer tissues (Figure 3B). To further confirm the mRNA expression of GNPAT1, the similar results was also found in two GEO cohorts (Figures 3C, D).

We also used UALCAN and HPA online database to identify protein levels of GNPAT1 in BRCA. Based on CPTAC database, protein expression level of GNPAT1 was elevated in BRCA tissues compared with normal tissues (Figure 3E). A higher level of expression of GNPAT1 protein was also found in the BRCA tissues than that in the normal tissues, as visualized by the representative IHC images from the HPA database (Figure 3F).





In conclusion, the mRNA and protein expression level of GNPAT1 were significantly elevated in BRCA tissues compared with normal breast tissues.

3.2 Validation of GNPAT1 expression in cell lines and clinical samples

To further identify the expression of GNPAT1, we conducted qRT-PCR and Western blot on different cell lines, including one non-transformed mammary epithelial cell line and six breast cancer cell lines. The results indicated that mRNA and protein expression

level of GNPAT1 was significantly elevated in breast cancer cell lines compared with mammary epithelial cell line (Figures 4A, B).

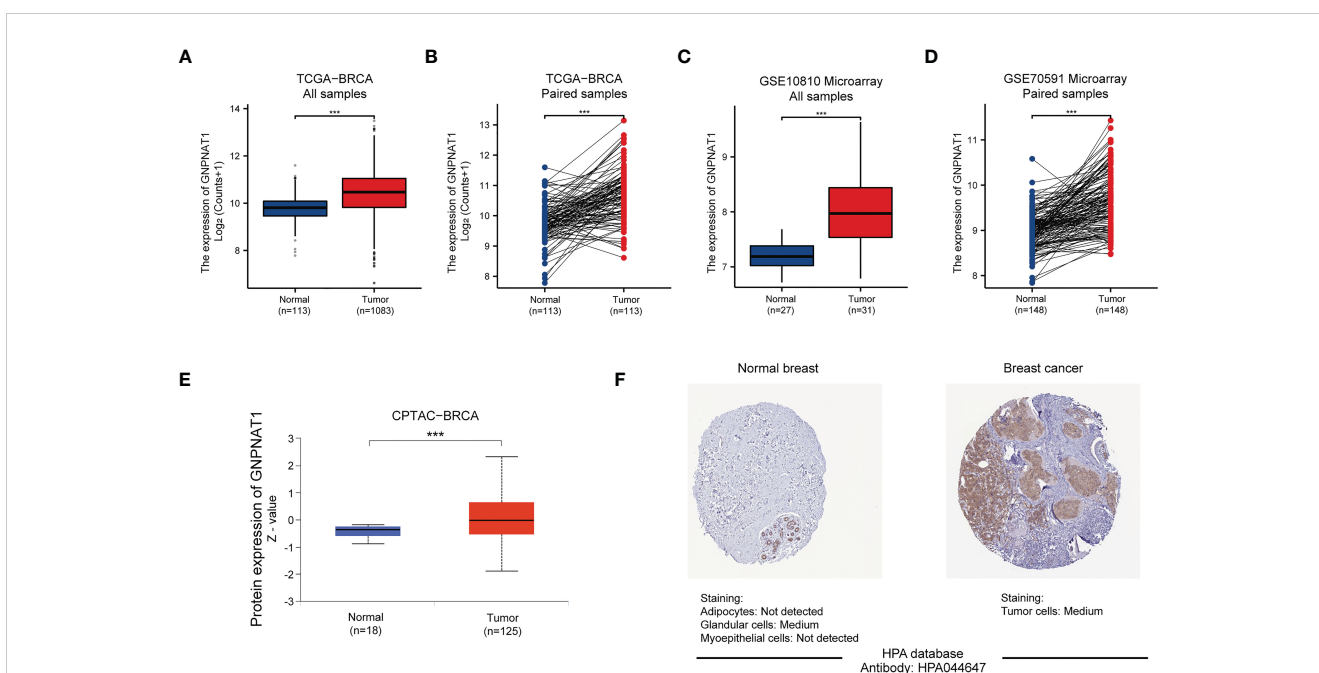
The IHC staining was carried out on a cohort comprising 16 cases of primary breast cancer tissues paired with para-tumor tissues, and the expression of GNPAT1 was up-regulated in 87.5% (14/16) of breast cancer tissues via IHC optical density score. Representative images of different subtypes were presented in Figure 4C separately, and quantization of results were shown in the right part.

These results indicated that the expression level of GNPAT1 was significantly up-regulated in every subtype of BRCA cell lines and clinical tissues, and up-regulation of GNPAT1 was not a specific subtype dependent.

3.3 Relationship between the expression level of GNPAT1 and hallmarks of BRCA

To determine the relationship between the expression of the GNPAT1 and hallmarks of BRCA, we firstly analyzed the clinical pathological characteristics of BRCA patients from TCGA. The mRNA expression level of the GNPAT1 was significantly correlated with the stage, tumor stage and node stage, but it was nothing to do with metastasis stage (Figure 5A-D).

Due to the above results, we subsequently validated the relationship between the expression level of GNPAT1 and proliferation and invasion abilities *in vitro*. We detected a serious of proteins related to cell proliferation and invasion. Knockdown of



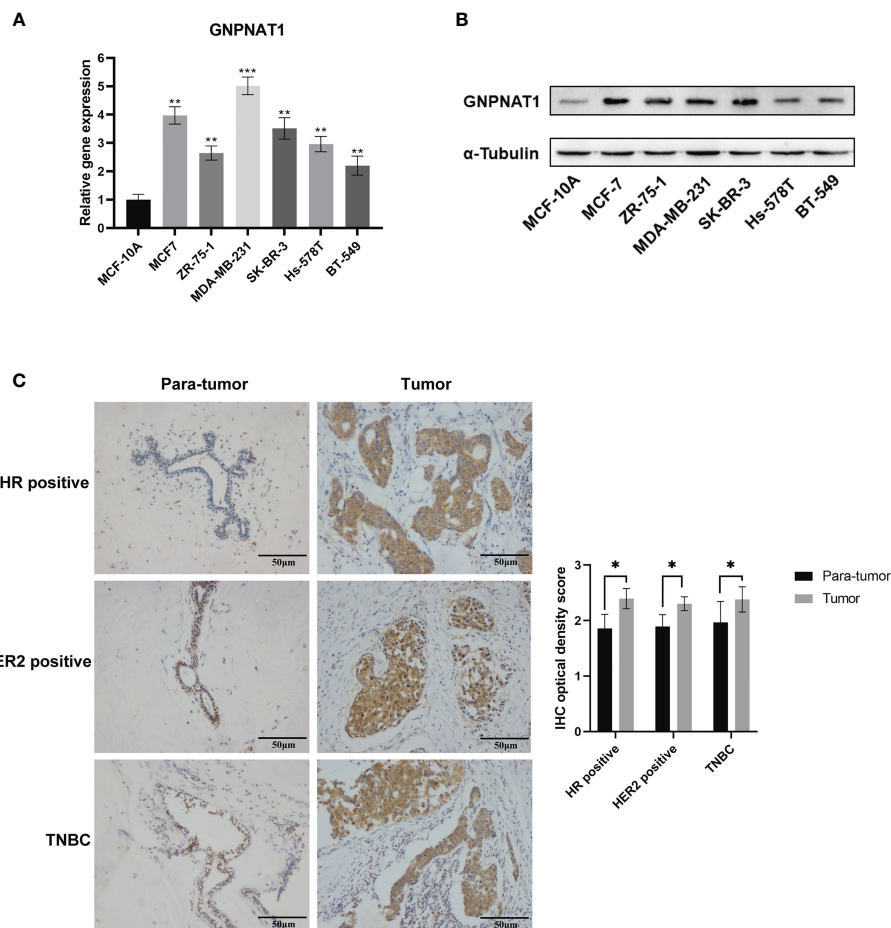


FIGURE 4

Validation of GNPAT1 expression in cell lines and clinical tissues samples. (A) qRT-PCR (Independent samples t-test) and (B) Western blot was conducted in different breast cancer cell lines. (C) Representative microscopic images (200x magnification, scale bar 50 μ m) demonstrate high expression of GNPAT1 in BRCA tissues confirmed by IHC; the result of quantification of GNPAT1 expression in IHC images is shown in the right part (Paired samples t-test). (*p-value < 0.05; **p-value < 0.01; ***p-value < 0.001).

GNPNAT1 decreased the expression of c-Myc, CyclinD1 and Bcl-2, while Bax was upregulated; meanwhile, N-cadherin and Vimentin were downregulated but E-cadherin was upregulated as the knockdown of GNPAT1 (Figure 5E). CCK-8 assay was used to detect the cell proliferation. As results indicated, knockdown of GNPAT1 remarkably impaired the proliferation of MDA-MB-231 and MCF-7 (Figures 5F, G). Transwell assay was used to detect the cell invasion. As we anticipated, knockdown of GNPAT1 attenuated the invasion of MDA-MB-231 and MCF-7 (Figure 5H).

To summarize, these results showed that GNPAT1 might be associated with tumor progression and regional lymph node metastasis in BRCA patients, and knockdown of GNPAT1 impairs the proliferation and invasion abilities of BRCA *in vitro*.

3.4 Potential diagnostic and prognostic value of GNPAT1 in BRCA

Since GNPAT1 was differentially expressed between breast cancer and normal tissues, we considered whether GNPAT1 had potential diagnostic and prognostic value in BRCA.

Firstly, we used ROC curves to verify the diagnostic value of GNPAT1. The results indicated that the area under the curve (AUC) of GNPAT1 was 0.756, 0.867, 0.794 for TCGA, GSE10810 and GSE70591 cohort respectively (Figures 6A–C). Also, we examined the expression of GNPAT1 at various stages in TCGA cohort with AUC values of 0.809, 0.812 and 0.837 for stages I, II, III and IV respectively (Figures 6D–F).

Furthermore, we analyzed the relationship between GNPAT1 expression and prognosis of BRCA patients via K-M plotter database. Compared with the low GNPAT1 expression group, the overall survive of the high GNPAT1 expression group exhibited a significantly worse prognosis (Figure 6G). In different subtypes of BRCA patients, HR positive and TNBC patients had a significantly worse prognosis, while HER2 patients were not (Figures 6H–J). In Supplement Figures 1A–D, we re-access survive curve of BRCA patients via GEPIA 2 database, and results indicate that HER2 patients also had a significantly worse prognosis.

In addition, we evaluated the prognostic effect of GNPAT1 expression in BRCA patients by using Cox regression analysis; in multicox analysis, GNPAT1 was found as an independent predictor for overall survival in BRCA patients (Figures 6K, L).

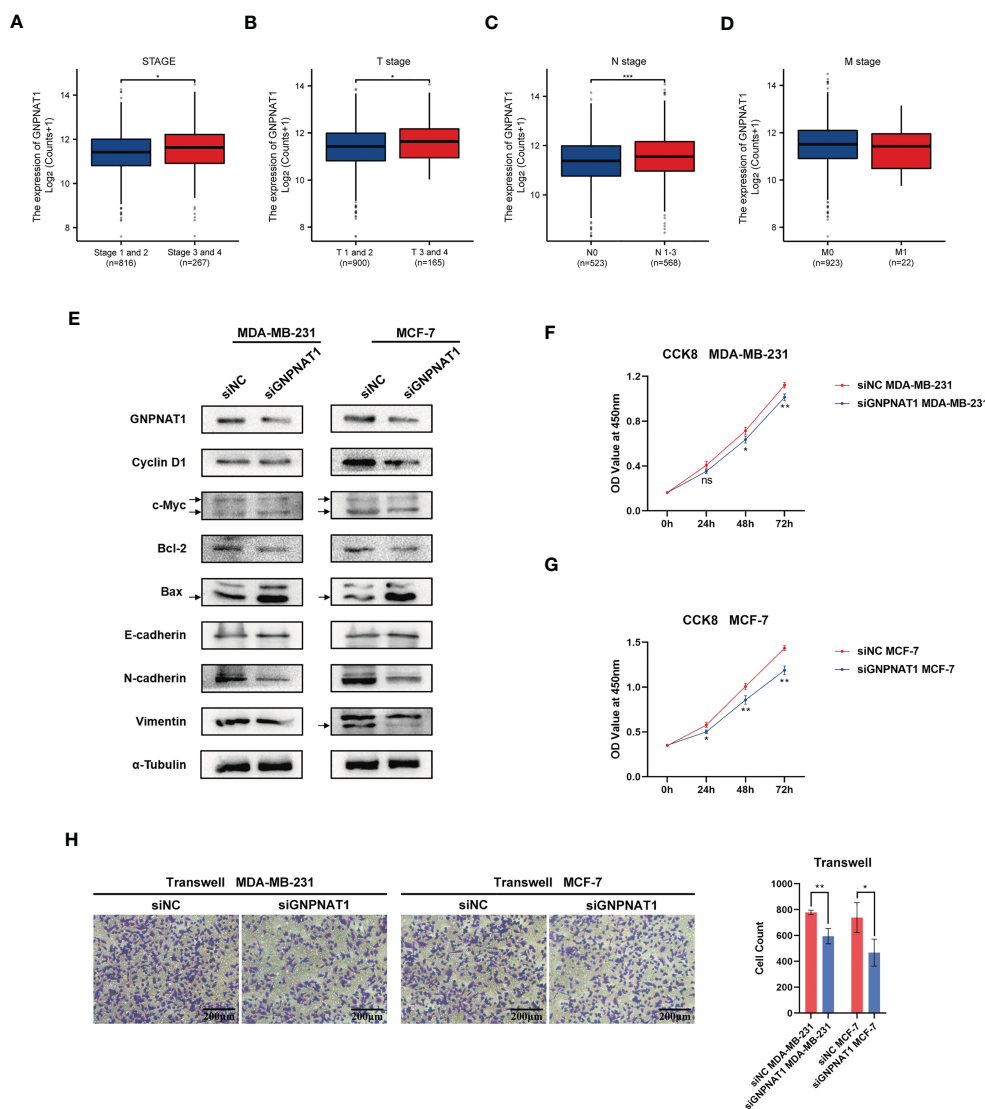


FIGURE 5
 Association between the expression level of GNPAT1 and hallmarks in BRCA. Association of GNPAT1 mRNA expression and (A) stage, (B) T stage, (C) N stage, (D) M stage from TCGA database (Wilcoxon rank sum test). (E) Effect of GNPAT1 knockdown on proliferation and invasion of MCF-7 and MDA-MB-231 were detected by Western blot analysis. Effect of GNPAT1 knockdown on proliferation of (F) MDA-MB-231 and (G) MCF-7 were detected by CCK-8 assay (Independent samples t-test). (H) Effect of GNPAT1 knockdown on invasion of MDA-MB-231 and MCF-7 were detected by Transwell assay (100x magnification, scale bar 200 μm), the result of cell counting is shown in the right part (Independent samples t-test). (*p-value < 0.05; **p-value < 0.01; ***p-value < 0.001).

These results suggested that GNPAT1 expression have potential to be a diagnostic and prognostic biomarker in BRCA patients.

3.5 Identification of DEGs in BRCA and functional inference analysis

To elucidate the potential mechanism of GNPAT1 in BRCA patients, we divided 1083 BRCA patients into two groups by the median expression level of GNPAT1. We totally identified 1877 DEGs including 57 up- and 1820 down- regulation DEGs (Figure 7A). Then, DEGs were analyzed using GO terms that

provide a context of cellular component (CC), molecular function (MF), and biological process (BP). The results revealed that DEGs were enriched in different GO terms such as humoral immune response, intermediate filament-based process and receptor ligand activity (Figure 7B). The KEGG pathway enrichment analysis revealed that neuroactive ligand-receptor interaction, protein digestion and absorption and estrogen signaling pathway is enriched in DEGs (Figure 7C).

Additionally, GSEA was conducted to find specific pathways for high GNPAT1 expression group and low GNPAT1 expression group. GSEA results showed that pathways of non-homologous end joining (NHEJ), mismatch repair, nucleotide excision repair, citrate cycle, N-Glycan biosynthesis and basal transcription factors

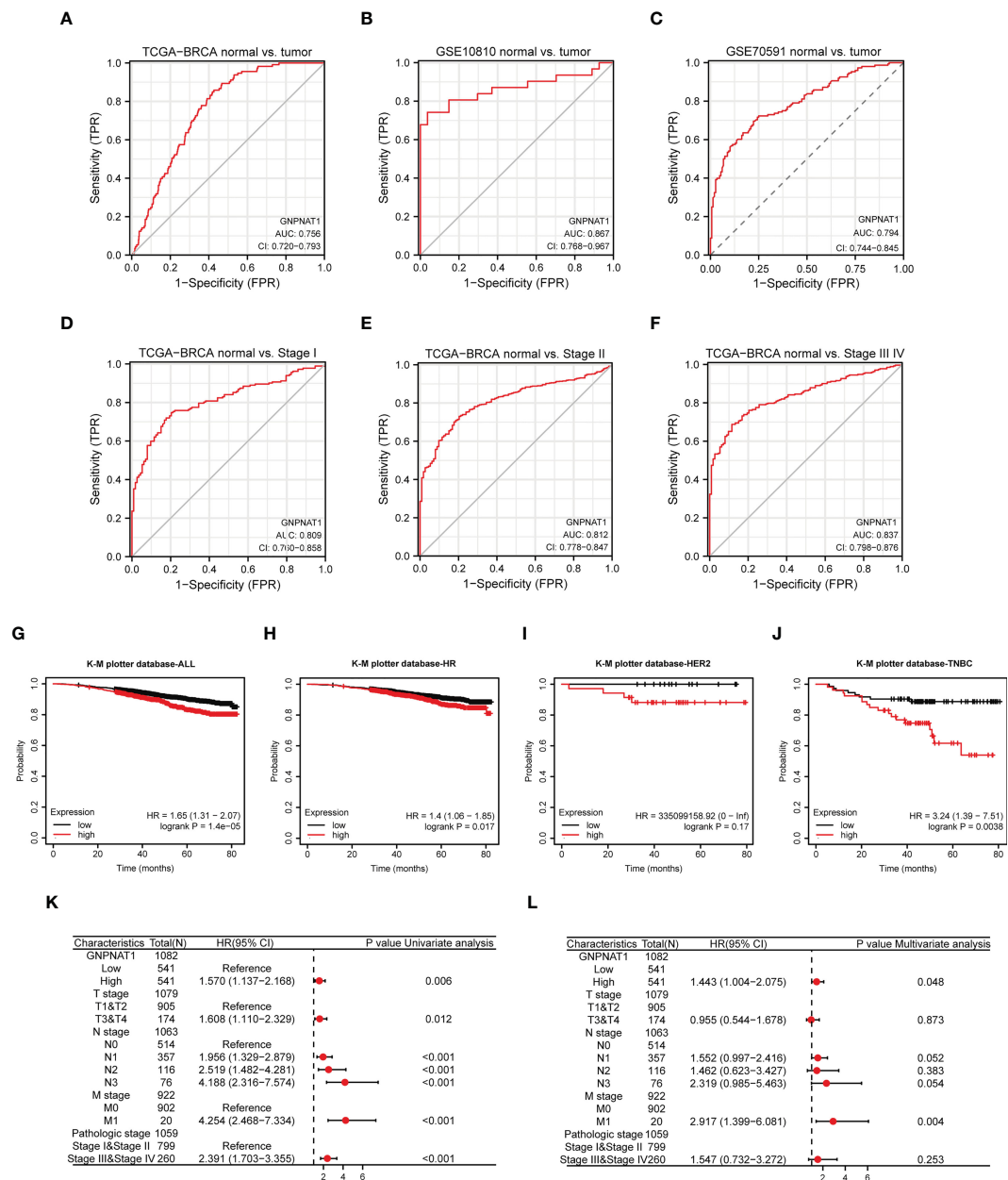


FIGURE 6 Potential clinical value of GNPAT1 in BRCA patients. (A–C) ROC curves of GNPAT1 expression in TCGA-BRCA and GEO cohorts. (D–F) ROC curves of GNPAT1 expression in TCGA-BRCA cohort with different pathological stages. The Kaplan–Meier curves about the correlation between GNPAT1 expression and overall survive of (G) all patients, (H) HR positive, (I) HER2 positive, and (J) TNBC of in TCGA database (Log-rank test) via K-M plotter. (K, L) Univariate and multivariate Cox analyses of GNPAT1 and pathological characteristics.

were significantly enriched in GNPAT1 high expression group, while arachidonic acid metabolism, linoleic acid metabolism and intestinal immune network for IgA production were enriched in GNPAT1 low expression group (Figure 7D).

In conclusion, more metabolism-related and DNA repair processes were enriched in the high GNPAT1 expression group, and more immune-related biological processes were found to be enriched in the low GNPAT1 expression group, suggesting that the high expression of GNPAT1 conferred an increased tumor proliferation and a decreased immune phenotype in BRCA.

3.6 GNPAT1 and the immune microenvironment in BRCA

To further investigate the relation between the expression of GNPAT1 and the decreased immune phenotype, we used ESTIMATE, CIBERSORT algorithm and TISIDB database to assess the immune level in BRCA cohort of TCGA.

ESTIMATE is a method that uses gene expression signatures to evaluate the levels of immune cell infiltration, stromal content score, stromal-immune comprehensive score and tumor purity for each

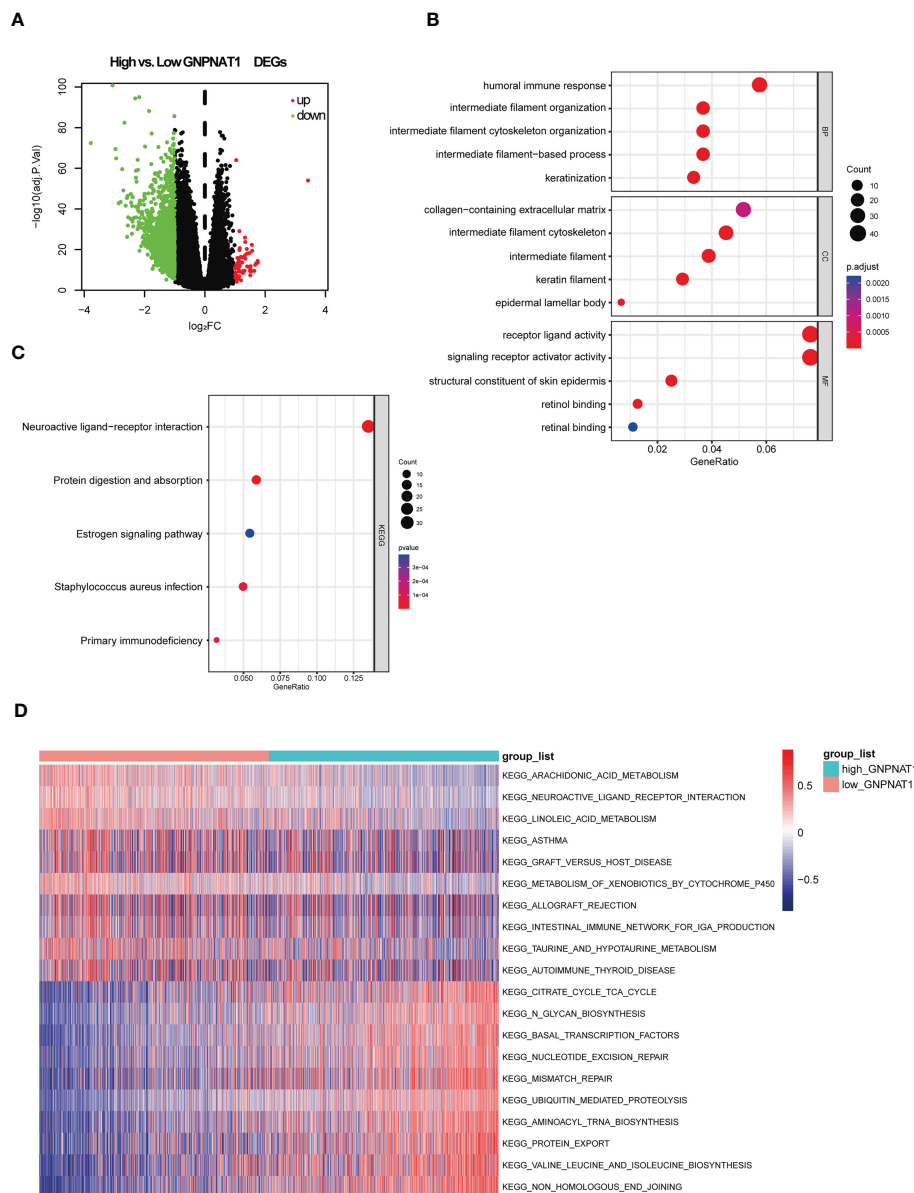


FIGURE 7 GNPAT1-related DEGs and functional enrichment analysis of GNPAT1 in breast cancer using GO, KEGG and GSVA. **(A)** Volcano plot of DEGs in high GNPAT1 group in TCGA-BRCA cohort compared with low GNPAT1 group. **(B)** Dot plot of the DEGs involving GO terms. **(C)** Dot plot of the DEGs involving KEGG pathways. **(D)** Heatmap of differentially expressed KEGG pathways through GSVA.

BRCA sample. The results of the ESTIMATE analyses suggested that the high GNPAT1 expression group had lower immune score and ESTIMATE score than the low GNPAT1 expression group, while the tumor purity score was higher (Figures 8A–D).

Then, we estimated the proportions of 22 distinct immune cell types using the CIBERSORT algorithm. The CIBERSORT analyses showed that expression of GNPAT1 has significant positive correlations with T cells CD4 memory resting, macrophages M2 and mast cells resting in BRCA, and has negative correlations with B cells memory, T cells CD8, T cells follicular helper, T cells regulator, NK cells activated (Figure 8E).

Furthermore, we investigated the relations between abundance of TILs, MHC molecule and expression of GNPAT1 via TISIDB

database. As shown in Figure 9, the expression of GNPAT1 was negatively associated with almost all TILs abundance and MHC molecule expression. Representative images of Pearson correlation analysis were also presented.

Nowadays immunotherapy targeting immune checkpoint is a rising field of TNBC treatment, so we also want to figure out the correlation between the expression of GNPAT1 and the efficacy of immune checkpoint inhibitors (ICIs) in TNBC patients. In TNBC from TCGA cohort, the group with high expression of GNPAT1 had increasing expression level of inhibitory immune checkpoints expression, such as CD274, Hepatitis A Virus Cellular Receptor 2 (HAVCR2), Programmed cell death1 (PDCD1), programmed cell death 1 ligand 2 (PDCD1LG2) and T cell immunoreceptor with Ig

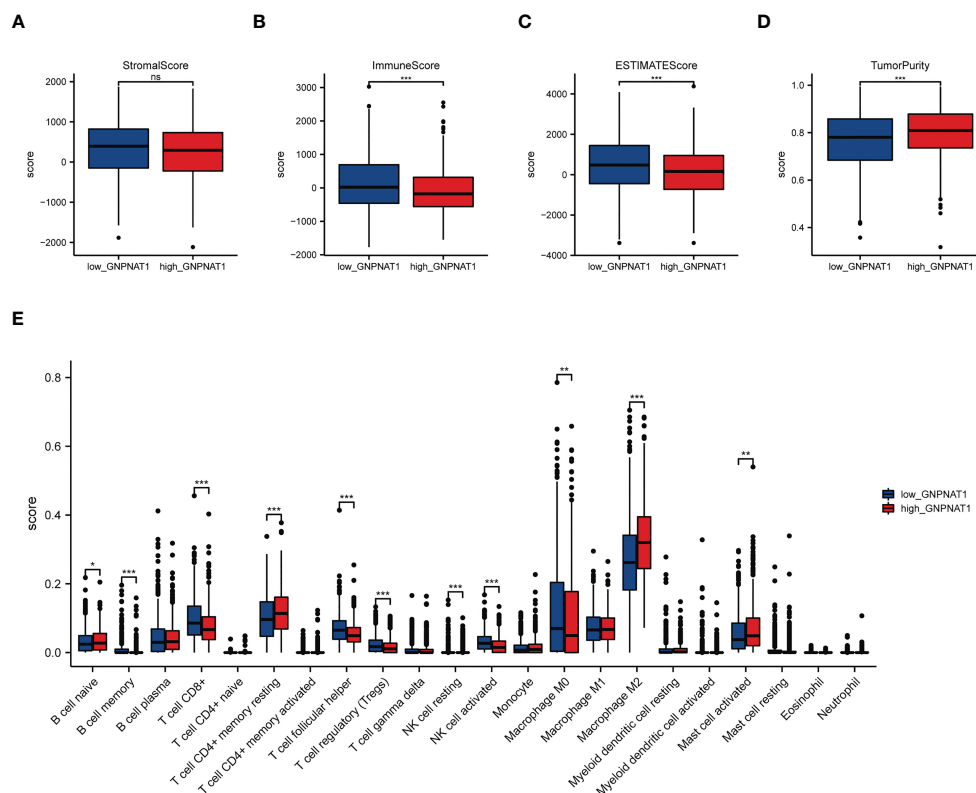


FIGURE 8

Correlation of GNPAT1 expression with immune infiltration level in BRCA. (A) Stromal scores, (B) Immune scores, (C) ESTIMATE scores, and (D) tumor purity between high GNPAT1 expression group and low GNPAT1 expression group (Wilcoxon rank sum test). (E) CIBERSORT analysis between the high GNPAT1 and low GNPAT1 group (Wilcoxon rank sum test). (*p-value < 0.05; **p-value < 0.01; ***p-value < 0.001). ns, not significant.

and ITIM domains (TIGIT) (Figure 10A), and also had a poor response to immunotherapy via TIDE algorithm (Figure 10B). Spearman correlation analysis revealed that the expression of GNPAT1 are positively correlated with the expression of CD274, PDCDLG2 and HAVCR2 (Figure 10C), and the expression of GNPAT1 was negatively correlated with the infiltration of follicular helper T cell, activated NK cell and CD8⁺ T cell in TNBC patients (Figure 10D).

Taken together, the expression of GNPAT1 was negatively associated with immune cell recruitment in BRCA, which possibly altered the composition of immune cells in the tumor environment and thereby affected the progression of BRCA patients. Patients with up-regulated GNPAT1 had low level of TILs infiltration and MHC abundance, and TNBC patients with up-regulated GNPAT1 had poor efficacy of immunotherapy in terms of ICIs.

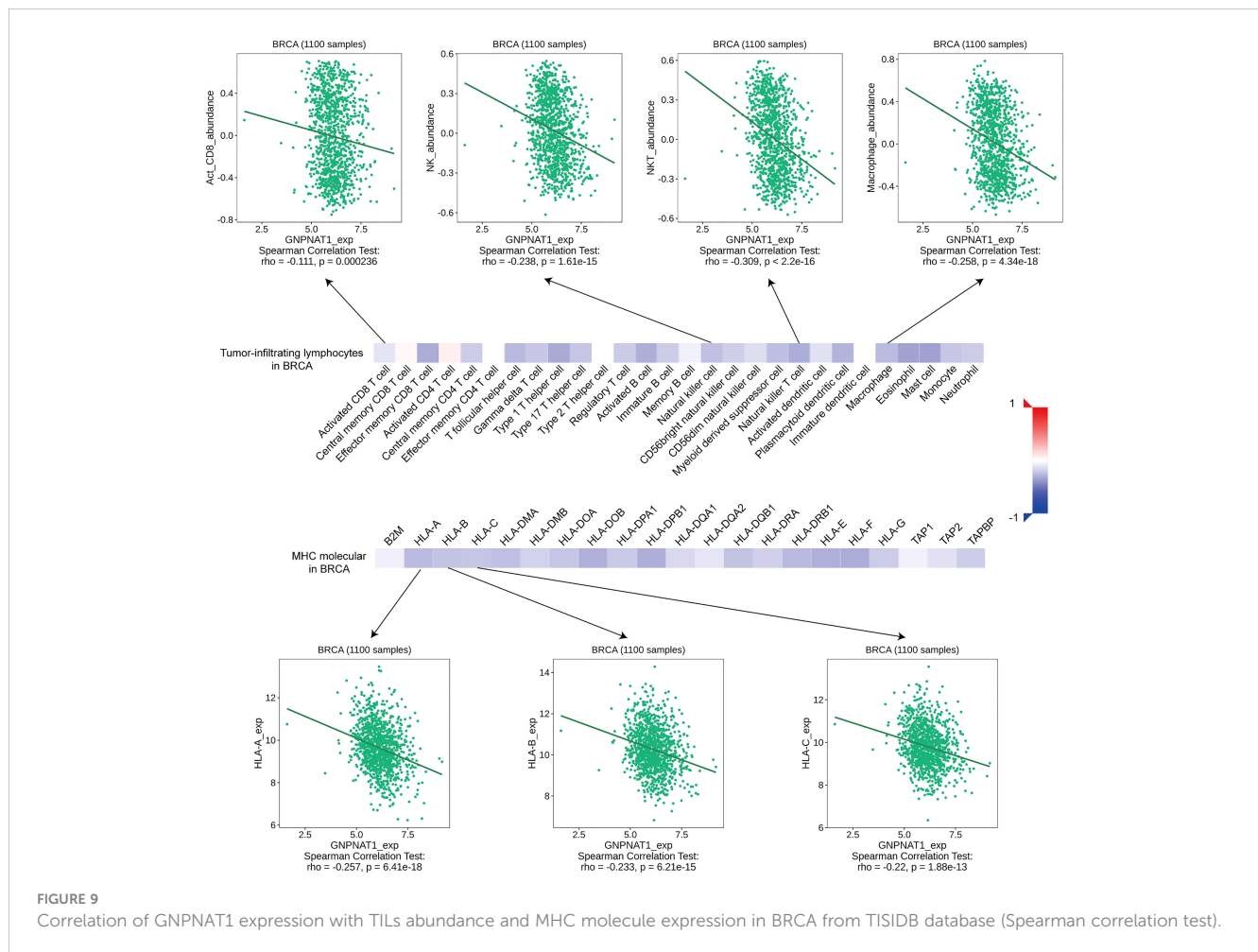
4 Discussion

In the previous study, researchers observed that GNPAT1 was significantly up-regulated in lung adenocarcinoma (9–11), and overexpression of GNPAT1 led to promote proliferative and metastatic ability of A549, a non-small cell lung cancer cells (22). Additionally, intracellular levels of GNPAT1 in ER positive breast cancer cell lines had the potential to predict sensitivity to

radiotherapy (8). However, there has no study regarding the clinical role and potential mechanism of GNPAT1 in BRCA.

In this study, we demonstrated that GNPAT1 was significantly overexpressed in nine out of the 23 human cancer tissues. Based on the ROC analyses, the diagnostic efficacy of GNPAT1 was proved in different cohorts, and AUC value highlighted the significant differences between the normal tissues and different tumor stages. In addition, GNPAT1 was found as an independent predictor for overall survival in BRCA patients. The following analyses also confirmed that higher GNPAT1 expression in BRCA was related to more unfavorable prognosis in BRCA patients. A high GNPAT1 expression was observed in BRCA from cell lines and clinical samples as well as TCGA and GEO datasets.

GNPAT1 is a protein with a crucial role in HBP, and HBP is a branch of carbohydrate metabolism which links glucose, amino acid, nucleotide and fatty acid metabolism. Except for increasing glucose consumption, tumor cells also enhanced the demand for glutamine, an essential substrate for HBP (23). Furthermore, the final product of HBP, UDP-GlcNAc, is an essential cell signal regulator and contributes to tumor growth. UDP-GlcNAc is then used for N-linked and O-linked glycosylation and for O-GlcNAcylation modification of nuclear and cytoplasmic proteins (24). O-GlcNAcylation, one type of post-translational modification, was prevalent in tumors, and enhancing O-GlcNAcylation



promotes DNA repair, proliferation, epithelial-mesenchymal transition, invasion and metastasis in BRCA (25–27). A study also reported that inhibition of HBP causes breast cancer growth arrest and apoptosis (28). Similar to this, our *in vitro* experiments have confirmed that knocking down GNPAT1 in breast cancer cell lines results in reduced proliferation and invasion capabilities of breast cancer cells. Similar to these, our *in vitro* experiments have indicated that knocking down GNPAT1 in breast cancer cell lines results in decreased proliferation and invasion capabilities of breast cancer cells. Our GSVA results also reminded that high GNPAT1 expression group was mainly enriched in the TCA cycle, NHEJ, mismatch repair, ubiquitin-mediated proteolysis and amino acid biosynthesis, in line with the above study, which proved our functional enrichment results are meaningful.

Tumor microenvironment, the basis of tumor growth and development, was infiltrated by immune cells (29). Our results reveal that GNPAT1 expression is negatively correlated with almost all TILs infiltration and MHCs abundance, which may suggest that high levels of GNPAT1 reduce the infiltration and antigen presentation of immune cells in BRCA. Tumor-associated macrophages playing a key role in shaping the tumor microenvironment (30). The prior reports pointed out that glucose metabolism promotes O-GlcNAcylation in macrophages to enhanced tumor invasion (31), and decreasing of O-GlcNAcylation lead to mitigating the immune-

suppressive program of M2 macrophages (32). Similarly, we explored that increasing expression of GNPAT1 has a positive correlation with M2 macrophages, while has a negative correlation with total macrophages, which possibly alters the composition of macrophages in the tumor environment and thereby affected the progression of BRCA patients.

ICIs enhance antitumor immunity mainly through overcome tumor cell-mediated immune inactivation, reverses immune tolerance, restores or strengthens the patient’s own anti-tumor immunity (33). The clinical experiments with the ICIs, such as anti-PD1/PD-L1 and anti-CTLA-4, alone or in combination with chemotherapy, has performed for TNBC patients, and some ICIs were approved for use as a means of clinical therapy (34). Increasing sensitivity of immunotherapy and predicting the outcome of immunotherapy are the hot topics recently. Previous study already proved that targeting HBP sensitizes pancreatic cancer to anti-PD1 therapy in pancreatic cancer (35), and O-GlcNAcylation inhibition activates T cell-mediated antitumor immunity *in vitro* (36). Our results point out that, in TNBC patients, high GNPAT1 expression are positively correlated with inhibitory immune checkpoints expression, such as CD274, PDCD1, PDCD1LG2, TIGIT, HAVCR2. Patients with high expression of immune checkpoints are more suitable for immunotherapy, but the results of TIDE algorithm revealed that TNBC patients with high

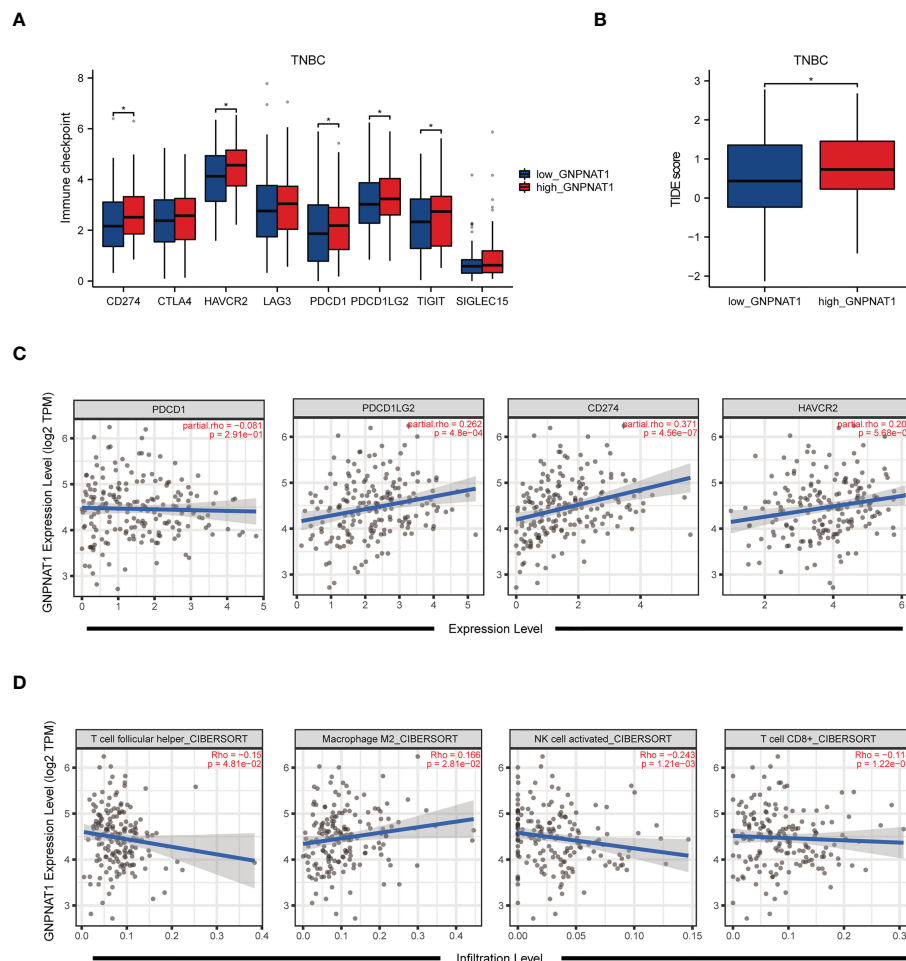


FIGURE 10

Correlation of GNPAT1 expression with immunotherapy response and immune microenvironment in TNBC. (A, B) Box plot showed the expression of immune checkpoints and TIDE score in patients with different expression of GNPAT1 in TNBC patients (Wilcoxon rank sum test). (C, D) Spearman correlation analysis between expression of GNPAT1 and expression levels of immune checkpoints and infiltration levels of immune cells (Spearman correlation test). (*p-value < 0.05).

GNPAT1 expression has poor immunotherapy efficacy. Hence, we speculate that the targeting GNPAT1 become an effective combined method to sensitize immunotherapy, and it even become a brand-new and universal anti-tumor therapy target in TNBC.

5 Conclusion

In summary, GNPAT1 was high expressed in BRCA, and the up-regulation was related to a poor prognosis. Our study suggests that GNPAT1 may serve as a diagnostic and prognostic biomarker and novel target for intervention in BRCA patients in the future. Our future study will focus on the mechanism of GNPAT1 in BRCA.

Data availability statement

The datasets presented in this study can be found in online repositories. The names of the repository/repositories and accession number(s) can be found within the article/Supplementary Material.

Author contributions

YZ and RY designed this study. RY, YW, HC, RZ and ZH performed bioinformatic analyses. RY and YZ performed the wet experiments and wrote the first draft of the manuscript. CC and TC funded and revised the manuscript. All authors contributed to the article and approved the submitted version.

Funding

This work was funded by the National Natural Science Foundation of China (Grant number: 82073255), and the Foundation of Chongqing Municipal Education Commission (Grant number: HZ2021006).

Acknowledgments

We thank for associate professor Zuo from the Chongqing Medical University and his valuable discussion.

Conflict of interest

The authors declare that the research was conducted in the absence of any commercial or financial relationships that could be construed as a potential conflict of interest.

Publisher's note

All claims expressed in this article are solely those of the authors and do not necessarily represent those of their affiliated

organizations, or those of the publisher, the editors and the reviewers. Any product that may be evaluated in this article, or claim that may be made by its manufacturer, is not guaranteed or endorsed by the publisher.

Supplementary material

The Supplementary Material for this article can be found online at: <https://www.frontiersin.org/articles/10.3389/fimmu.2023.1152678/full#supplementary-material>

References

- Sung H, Ferlay J, Siegel RL, Laversanne M, Soerjomataram I, Jemal A, et al. Global cancer statistics 2020: GLOBOCAN estimates of incidence and mortality worldwide for 36 cancers in 185 countries. *CA Cancer J Clin* (2021) 71(3):209–49. doi: 10.3322/caac.21660
- Cancer Genome Atlas N. Comprehensive molecular portraits of human breast tumours. *Nature* (2012) 490(7418):61–70. doi: 10.1038/nature11412
- Perou CM, Sørlie T, Eisen MB, van de Rijn M, Jeffrey SS, Rees CA, et al. Molecular portraits of human breast tumours. *Nature* (2000) 406(6797):747–52. doi: 10.1038/35021093
- Waks AG, Winer EP. Breast cancer treatment: a review. *Jama* (2019) 321(3):288–300. doi: 10.1001/jama.2018.19323
- McDonald ES, Clark AS, Tchou J, Zhang P, Freedman GM. Clinical diagnosis and management of breast cancer. *J Nucl Med* (2016) 57(Suppl 1):9s–16s. doi: 10.2967/jnumed.115.157834
- Wang J, Liu X, Liang YH, Li LF, Su XD. Acceptor substrate binding revealed by crystal structure of human glucosamine-6-phosphate n-acetyltransferase 1. *FEBS Lett* (2008) 582(20):2973–8. doi: 10.1016/j.febslet.2008.07.040
- Mio T, Yamada-Okabe T, Arisawa M, Yamada-Okabe H. Saccharomyces cerevisiae GNA1, an essential gene encoding a novel acetyltransferase involved in UDP-n-acetylglucosamine synthesis. *J Biol Chem* (1999) 274(1):424–9. doi: 10.1074/jbc.274.1.424
- Meehan J, Gray M, Martinez-Perez C, Kay C, Wills JC, Kunkler IH, et al. A novel approach for the discovery of biomarkers of radiotherapy response in breast cancer. *J Pers Med* (2021) 11(8):796. doi: 10.3390/jpm11080796
- Liu W, Jiang K, Wang J, Mei T, Zhao M, Huang D. Upregulation of GNPAT1 predicts poor prognosis and correlates with immune infiltration in lung adenocarcinoma. *Front Mol Biosci* (2021) 8:605754. doi: 10.3389/fmolb.2021.605754
- Zhu P, Gu S, Huang H, Zhong C, Liu Z, Zhang X, et al. Upregulation of glucosamine-phosphate n-acetyltransferase 1 is a promising diagnostic and predictive indicator for poor survival in patients with lung adenocarcinoma. *Oncol Lett* (2021) 21(6):488. doi: 10.3892/ol.2021.12750
- Ding P, Peng B, Li G, Sun X, Wang G. Glucosamine-phosphate n-acetyltransferase 1 and its DNA methylation can be biomarkers for the diagnosis and prognosis of lung cancer. *J Clin Lab Anal* (2022) 36(9):e24628. doi: 10.1002/jcla.24628
- Robin X, Turck N, Hainard A, Tiberti N, Lisacek F, Sanchez JC, et al. pROC: an open-source package for r and s+ to analyze and compare ROC curves. *BMC Bioinf* (2011) 12:77. doi: 10.1186/1471-2105-12-77
- Love MI, Huber W, Anders S. Moderated estimation of fold change and dispersion for RNA-seq data with DESeq2. *Genome Biol* (2014) 15(12):550. doi: 10.1186/s13059-014-0550-8
- Yu G, Wang LG, Han Y, He QY. clusterProfiler: an R package for comparing biological themes among gene clusters. *Omic* (2012) 16(5):284–7. doi: 10.1089/omi.2011.0118
- Hänzelmann S, Castelo R, Guinney J. GSEA: gene set variation analysis for microarray and RNA-seq data. *BMC Bioinf* (2013) 14:7. doi: 10.1186/1471-2105-14-7
- Smyth GK. Linear models and empirical bayes methods for assessing differential expression in microarray experiments. *Stat Appl Genet Mol Biol* (2004) 3:Article3. doi: 10.2202/1544-6115.1027
- Yoshihara K, Shahmoradgoli M, Martínez E, Vegesna R, Kim H, Torres-García W, et al. Inferring tumour purity and stromal and immune cell admixture from expression data. *Nat Commun* (2013) 4:2612. doi: 10.1038/ncomms3612
- Newman AM, Steen CB, Liu CL, Gentles AJ, Chaudhuri AA, Scherer F, et al. Determining cell type abundance and expression from bulk tissues with digital cytometry. *Nat Biotechnol* (2019) 37(7):773–82. doi: 10.1038/s41587-019-0114-2
- Jiang P, Gu S, Pan D, Fu J, Sahu A, Hu X, et al. Signatures of T cell dysfunction and exclusion predict cancer immunotherapy response. *Nat Med* (2018) 24(10):1550–8. doi: 10.1038/s41591-018-0136-1
- Vandesompele J, De Preter K, Pattyn F, Poppe B, Van Roy N, De Paeppe A, et al. Accurate normalization of real-time quantitative RT-PCR data by geometric averaging of multiple internal control genes. *Genome Biol* (2002) 3(7):Research0034. doi: 10.1186/gb-2002-3-7-research0034
- Varghese F, Bukhari AB, Malhotra R, De A. IHC profiler: an open source plugin for the quantitative evaluation and automated scoring of immunohistochemistry images of human tissue samples. *PLoS One* (2014) 9(5):e96801. doi: 10.1371/journal.pone.0096801
- Feng Y, Li N, Ren Y. GNPAT1 predicts poor prognosis and cancer development in non-small cell lung cancer. *Cancer Manag Res* (2022) 14:2419–28. doi: 10.2147/CMARS367857
- van Geldermalsen M, Wang Q, Nagarajah R, Marshall AD, Thoeng A, Gao D, et al. ASCT2/SLC1A5 controls glutamine uptake and tumour growth in triple-negative basal-like breast cancer. *Oncogene* (2016) 35(24):3201–8. doi: 10.1038/onc.2015.381
- Akella NM, Ciraku L, Reginato MJ. Fueling the fire: emerging role of the hexosamine biosynthetic pathway in cancer. *BMC Biol* (2019) 17(1):52. doi: 10.1186/s12915-019-0671-3
- Chokchaitaweek C, Kobayashi T, Izumikawa T, Itano N. Enhanced hexosamine metabolism drives metabolic and signaling networks involving hyaluronan production and O-GlcNAcylation to exacerbate breast cancer. *Cell Death Dis* (2019) 10(11):803. doi: 10.1038/s41419-019-2034-y
- Zhang N, Zhu T, Yu K, Shi M, Wang X, Wang L, et al. Elevation of O-GlcNAc and GFAT expression by nicotine exposure promotes epithelial-mesenchymal transition and invasion in breast cancer cells. *Cell Death Dis* (2019) 10(5):343. doi: 10.1038/s41419-019-1577-2
- Efimova EV, Appelbe OK, Ricco N, Lee SS, Liu Y, Wolfgeher DJ, et al. O-GlcNAcylation enhances double-strand break repair, promotes cancer cell proliferation, and prevents therapy-induced senescence in irradiated tumors. *Mol Cancer Res* (2019) 17(6):1338–50. doi: 10.1158/1541-7786.MCR-18-1025
- Ricciardiello F, Votta G, Palorini R, Raccagni I, Brunelli L, Paiotta A, et al. Inhibition of the hexosamine biosynthetic pathway by targeting PGM3 causes breast cancer growth arrest and apoptosis. *Cell Death Dis* (2018) 9(3):377. doi: 10.1038/s41419-018-0405-4
- Hinshaw DC, Shevde LA. The tumor microenvironment innately modulates cancer progression. *Cancer Res* (2019) 79(18):4557–66. doi: 10.1158/0008-5472.CAN-18-3962
- Vitale I, Manic G, Coussens LM, Kroemer G, Galluzzi L. Macrophages and metabolism in the tumor microenvironment. *Cell Metab* (2019) 30(1):36–50. doi: 10.1016/j.cmet.2019.06.001
- Shi Q, Shen Q, Liu Y, Shi Y, Huang W, Wang X, et al. Increased glucose metabolism in TAMs fuels O-GlcNAcylation of lysosomal cathepsin b to promote cancer metastasis and chemoresistance. *Cancer Cell* (2022) 40(10):1207–22.e10. doi: 10.1016/j.ccell.2022.08.012
- Hinshaw DC, Hanna A, Lama-Sherpa T, Metge B, Kammerud SC, Benavides GA, et al. Hedgehog signaling regulates metabolism and polarization of mammary tumor-associated macrophages. *Cancer Res* (2021) 81(21):5425–37. doi: 10.1158/0008-5472.CAN-20-1723
- Bagchi S, Yuan R, Engleman EG. Immune checkpoint inhibitors for the treatment of cancer: clinical impact and mechanisms of response and resistance. *Annu Rev Pathol* (2021) 16:223–49. doi: 10.1146/annurev-pathol-042020-042741
- Peyraud F, Italiano A. Combined PARP inhibition and immune checkpoint therapy in solid tumors. *Cancers (Basel)* (2020) 12(6):1502. doi: 10.3390/cancers12061502

35. Sharma NS, Gupta VK, Garrido VT, Hadad R, Durden BC, Kesh K, et al. Targeting tumor-intrinsic hexosamine biosynthesis sensitizes pancreatic cancer to anti-PD1 therapy. *J Clin Invest* (2020) 130(1):451–65. doi: 10.1172/JCI127515

36. Zhu Q, Wang H, Chai S, Xu L, Lin B, Yi W, et al. O-GlcNAcylation promotes tumor immune evasion by inhibiting PD-L1 lysosomal degradation. *Proc Natl Acad Sci USA* (2023) 120(13):e2216796120. doi: 10.1073/pnas.2216796120